2-Bromo-1,3-bis[2-(2-naphthyl)vinyl]-benzene benzene hemisolvate and 9-bromodinaphth[1,2-a:2′,1′-j]anthracene

Joel T. Mague,[a]* J. Matthew Chudomel[b] and Paul M. Lahti[b]

[a]Department of Chemistry, Tulane University, New Orleans, LA 70118, USA, and [b]Department of Chemistry, University of Massachusetts, Amherst, MA 01003, USA
Correspondence e-mail: joelt@tulane.edu

2-Bromo-1,3-bis[2-(2-naphthyl)vinyl]benzene benzene hemisolvate, $C_{30}H_{21}Br \cdot 0.5C_6H_6$, (I), with two formula units in the asymmetric unit, exists in the crystal structure in a conformation in which the *trans* (2-naphthyl)vinyl substituents on the central bromobenzene moiety appear as nearly fully extended 'wings', while 9-bromodinaphth[1,2-a:2′,1′-j]anthracene, $C_{30}H_{17}Br$, (II), adopts a highly nonplanar 'manta-ray' shape, with the H atoms in the interior of the molecule within van der Waals contact distances. The packing of the significantly twisted molecules of (I) generates large voids which are filled by benzene solvent molecules, while molecules of (II) stack compactly with all C—Br bonds parallel within the stack.

Comment

9-Bromodinaphth[1,2-a:2′,1′-j]anthracene, (II), has been studied as a model for coronaphenes, a subset of the benzannelated annulene family of polycyclic aromatic hydrocarbons (PAHs) (Wilcox *et al.*, 1978). As part of this work, molecular mechanics computations (Lahti, 1988) were performed which indicated the presence of a Clar-type (Clar, 1964, 1972) localized structure, rather than extensive superaromatic delocalization around the perimeter. The previous study also envisaged using the reactivity of the Br atom at the 9-position to connect a strongly nonplanar PAH to other functionalities at this site, with the expectation that its presence would have a significant effect on the packing of such derivatives in the solid state. To confirm the predictions of the earlier molecular mechanics calculations, the structure of (II) was determined at low temperature to obtain accurate C—C bond distances, as well as to provide a benchmark for the crystal packing of derivatives of (II).

Compound (II) was readily prepared by the solution photocyclization of 2-bromo-1,3-bis[2-(2-naphthyl)vinyl]benzene, (I). The ease of photocyclization of (I) to form (II)

requires (I) to undergo *cis–trans* isomerization with conformational flexibility in solution, so it was also of interest to determine the solid-state structure of (I).
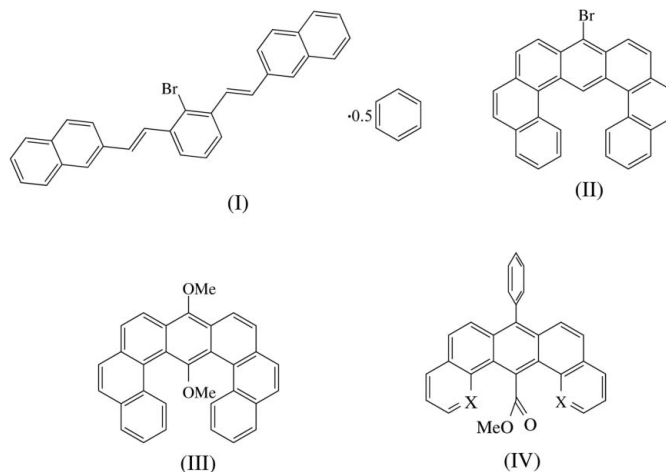

In the crystal structure, (I) exists in an extended (vinyl groups and *ipso*-C atoms of the naphthyl groups close to coplanarity with the central six-membered ring), though significantly twisted, conformation (Fig. 1) for each of the two independent molecules in the asymmetric unit. The primary difference between these is different orientations of the naphthyl groups with respect to the central six-membered ring. The dihedral angle between the mean planes of the naphthyl groups in (I) is 52.7 (5)° for molecule 1, while in molecule 2 it is 55.7 (5)°. As shown in Fig. 2, the packing consists of offset stacks of molecules with interdigitated ends, such that there are significant C—H···π interactions in the interdigitated region. Close contacts include C11—H11··· $Cg1(1 - x, 1 - y, 1 - z)$ (H···Cg = 2.70 Å and C—H···Cg = 148°), C27—H27···$Cg2(\frac{3}{2} - x, -\frac{1}{2} + y, \frac{3}{2} - z)$ (2.72 Å and 149°), C43—H43···$Cg3(\frac{1}{2} - x, \frac{1}{2} + y, \frac{3}{2} - z)$ (2.70 Å and 149°) and C57—H57···$Cg4(1 - x, -y, 1 - z)$ (2.77 Å and 157°) ($Cg1$–$Cg4$ are the centroids of the C39—C48, C9—C18, C51—C52 and C21—C22 bonds, respectively). As is evident from Table 1, there is a distinct alternation of C—C bond distances in the naphthyl groups (listed in full for the naphthyl group consisting of atoms C9–C18; the others show comparable values), indicating a concentration of π density in the shorter bonds and thereby favoring the formation of C—H···π interactions with individual C—C bonds rather than with the six-membered ring as a whole. This manner of packing leaves relatively large voids between the stacks, which are filled by benzene solvent molecules.

Compound (II) adopts a 'manta-ray'-shaped conformation in the crystal structure (Fig. 3b), presumably in part due to attempted relief of the structurally constrained close contacts between three H atoms in the interior of the molecule (H12···H16 = 2.01 Å, H12···H28 = 2.14 Å and H16···H28 = 1.89 Å). This conformation lends itself to efficient packing in the crystal structure, as shown in Fig. 4, with an offset π-stacking involving the C3–C7 portion of one molecule with the C1/C17/C18/C29/C30 portion of an adjacent molecule and with the C—Br bonds parallel. The interplanar contact

organic compounds
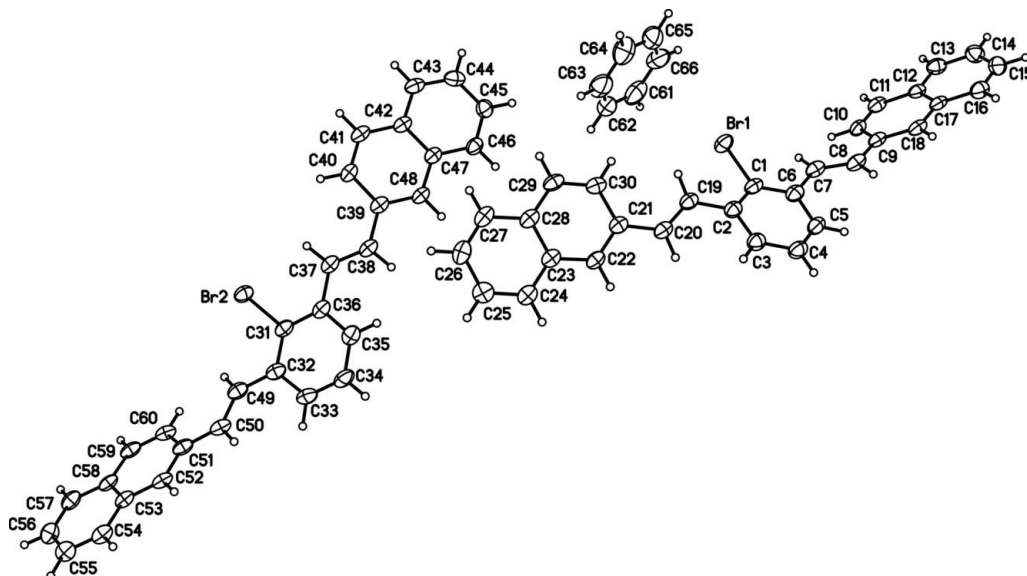
Figure 1
A perspective view of the asymmetric unit of (I), with displacement ellipsoids drawn at the 50% probability level.
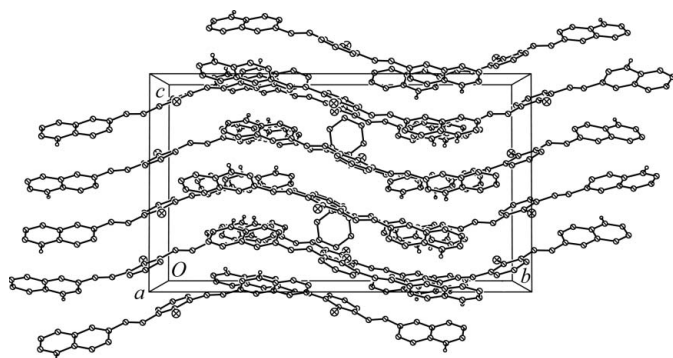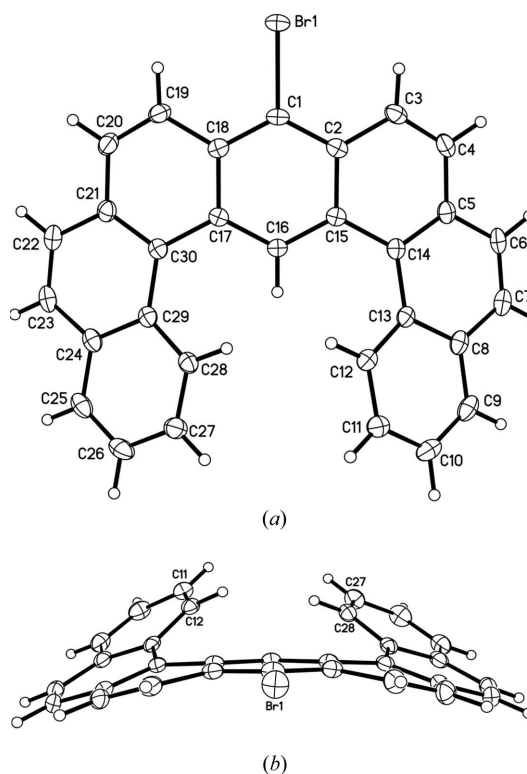

Figure 2
The packing in (I), viewed down *a*. Only those H atoms involved in the C—H···π interactions are included.

distance is about 3.36 Å. In addition, adjacent zigzag stacks with opposite concavity and C—Br bond orientation are connected *via* C—H···π interactions involving C23—H23 and the centroid ($Cg5$) of the C28—C29 bond in a neighboring stack [H23···$Cg5^i$ = 2.77 Å and C23—H23···$Cg5^i$ = 159°; symmetry code: (i) x, $-y + \frac{1}{2}$, $z - \frac{1}{2}$]. Additionally, there are attractive interstack C—H···Br interactions [H20···Br1^{ii} = 2.90 Å and C20—H20···Br1^{ii} = 159°; symmetry code: (ii) $-x + 1$, $y - \frac{1}{2}$, $-z + \frac{1}{2}$] (Brammer *et al.*, 2001).

The distinct alternation of C—C bond lengths of (II) in the two wings (Table 2) confirms the results of the earlier molecular mechanics calculations. Those computations also showed that a helical C_2 structure for (II) had a slightly lower energy than the approximate C_s structure found in the solid state. The earlier structural computations were confirmed as part of the present work by RB3LYP/6-31G*, RB3LYP/cc-pVDZ//6-31G* and RB3LYP/cc-pVDZ hybrid density functional computations on (II) using *GAUSSIAN03* (Frisch *et al.*, 2004), which show that the C_2 geometry is more stable than the C_s geometry by, respectively, 10.0, 10.9 and 10.5 kJ mol^{-1}

(no zero-point energy corrections). We presume that this slight energy difference is overcome by the more favorable packing afforded by the C_s geometry. The effective 'thickness' of the observed conformation is *ca* 2 Å, while that of the helical geometry would be *ca* 4 Å. The effective 'filled space' in the structure of (II) is 73.7%.

Figure 3
(*a*) A perspective view of the molecular structure of (II), with displacement ellipsoids drawn at the 50% probability level. (*b*) A view of (II) along the Br1—C1 bond.
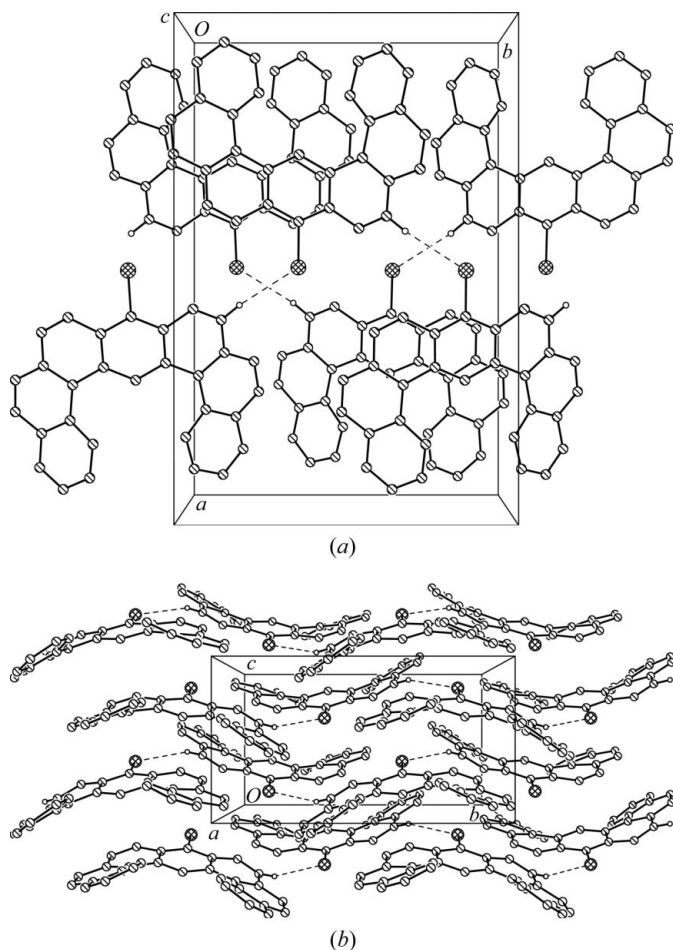
Figure 4
(a) The packing in (II), viewed down c. (b) The packing in (II), viewed approximately down a. Only H atoms involved in C—H···Br interactions are included.

In what appears to be the only crystal structure of an analogous compound reported to date, 9,18-dimethoxy-naphth[1,2-a:2′,1′-j]anthracene, (III) (Gupta *et al.*, 1991), was also found to have a C_s rather than a helical structure, with a computationally estimated preference of 14.2 kJ mol^{-1}. It is tempting to suggest that the increase in internal congestion as a result of replacing atom H16 by a methoxy group forces a preference for the C_s geometry. However, the similar compounds, (IV) (see scheme; X = CH, N) (Zimmerman & Wilson, 1992), have helical conformations. We think that these comparison cases support the notion that the helical and C_s conformations are sufficiently similar in energy that which one will be found in the solid state in any particular instance will be dependent on packing forces.

Experimental

Compounds (I) and (II) were prepared and purified according to the published method of Wilcox *et al.* (1978). X-ray quality crystals of (I) were obtained by the slow evaporation of a benzene–methanol solution (1:1 *v/v*) of the compound, while for (II), slow diffusion of hexane into a chloroform solution was used.

Table 1
Selected bond lengths (Å) for (I).

C7—C8	1.346 (4)	C14—C15	1.405 (4)
C9—C18	1.378 (4)	C15—C16	1.363 (4)
C9—C10	1.432 (4)	C16—C17	1.412 (4)
C10—C11	1.357 (4)	C17—C18	1.412 (4)
C11—C12	1.417 (4)	C19—C20	1.330 (4)
C12—C13	1.411 (4)	C21—C22	1.383 (4)
C12—C17	1.424 (4)	C39—C48	1.380 (4)
C13—C14	1.359 (4)	C51—C52	1.379 (4)

Compound (I)

Crystal data

C$_{30}$H$_{21}$Br·0.5C$_6$H$_6$	$V = 4724.7$ (7) Å^3
$M_r = 500.43$	$Z = 8$
Monoclinic, $P2_1/n$	Mo $K\alpha$ radiation
$a = 11.633$ (1) Å	$\mu = 1.76$ mm^{-1}
$b = 26.665$ (2) Å	$T = 100$ K
$c = 15.2364$ (14) Å	$0.36 \times 0.14 \times 0.03$ mm
$\beta = 91.513$ (1)°	

Data collection

Bruker SMART APEX CCD area-detector diffractometer	39415 measured reflections
	10288 independent reflections
Absorption correction: integration (*SADABS*; Sheldrick, 2008a)	7141 reflections with $I > 2\sigma(I)$
$T_{min} = 0.501$, $T_{max} = 0.956$	$R_{int} = 0.051$

Refinement

$R[F^2 > 2\sigma(F^2)] = 0.043$	613 parameters
$wR(F^2) = 0.101$	H-atom parameters constrained
$S = 1.01$	$\Delta\rho_{max} = 0.52$ e Å^{-3}
10288 reflections	$\Delta\rho_{min} = -0.67$ e Å^{-3}

Compound (II)

Crystal data

C$_{30}$H$_{17}$Br	$V = 1915.5$ (4) Å^3
$M_r = 457.35$	$Z = 4$
Monoclinic, $P2_1/c$	Mo $K\alpha$ radiation
$a = 19.749$ (3) Å	$\mu = 2.16$ mm^{-1}
$b = 13.2672$ (17) Å	$T = 100$ K
$c = 7.3108$ (9) Å	$0.16 \times 0.07 \times 0.04$ mm
$\beta = 90.021$ (2)°	

Table 2
Selected bond lengths (Å) for (II).

C3—C4	1.342 (3)	C16—C17	1.399 (3)
C4—C5	1.431 (3)	C17—C30	1.471 (3)
C5—C14	1.404 (3)	C19—C20	1.348 (3)
C5—C6	1.427 (3)	C20—C21	1.429 (3)
C6—C7	1.351 (3)	C21—C30	1.406 (3)
C7—C8	1.423 (3)	C21—C22	1.427 (3)
C8—C9	1.415 (3)	C22—C23	1.351 (3)
C8—C13	1.430 (3)	C23—C24	1.420 (3)
C9—C10	1.368 (3)	C24—C25	1.419 (3)
C10—C11	1.404 (3)	C24—C29	1.433 (3)
C11—C12	1.377 (3)	C25—C26	1.365 (3)
C12—C13	1.414 (3)	C26—C27	1.404 (3)
C13—C14	1.450 (3)	C27—C28	1.376 (3)
C14—C15	1.462 (3)	C28—C29	1.415 (3)
C15—C16	1.403 (3)	C29—C30	1.453 (3)

organic compounds

H atoms were placed in calculated positions, with C—H = 0.95 Å, and included as riding, with $U_{iso}(H) = 1.2U_{eq}(C)$.

For both compounds, data collection: *APEX2* (Bruker, 2009); cell refinement: *SAINT* (Bruker, 2009); data reduction: *SAINT*; program(s) used to solve structure: *SHELXTL* (Sheldrick, 2008*b*); program(s) used to refine structure: *SHELXTL*; molecular graphics: *SHELXTL*; software used to prepare material for publication: *SHELXTL*.

References

Brammer, L., Bruton, E. A. & Sherwood, P. (2001). *Cryst. Growth Des.* **1**, 277–290.
Bruker (2009). *APEX2* (Version 2009.11-0) and *SAINT* (Version 7.68A). Bruker AXS Inc., Madison, Wisconsin, USA.
Clar, E. (1964). *Polycyclic Hydrocarbons*, Vols. I and II. New York: Academic Publishers Inc.
Clar, E. (1972). In *The Aromatic Sextet*. London: John Wiley and Sons.
Frisch, M. J., *et al.* (2004). *GAUSSIAN03*. Revision B.03. Gaussian Inc., Wallingford, Connecticut, USA.
Gupta, R. B., Kaloustian, M. K., Franck, R. W. & Blount, J. F. (1991). *J. Am. Chem. Soc.* **113**, 359–361.
Lahti, P. M. (1988). *J. Org. Chem.* **53**, 4590–4593.
Sheldrick, G. M. (2008*a*). *SADABS*. Version 2008/2. University of Göttingen, Germany.
Sheldrick, G. M. (2008*b*). *Acta Cryst.* A**64**, 112–122.
Wilcox, C. F. Jr, Lahti, P. M., Rocca, J. R., Halpern, M. B. & Meinwald, J. (1978). *Tetrahedron Lett.* pp. 1893–1896.
Zimmerman, S. C. & Wilson, S. R. (1992). *Acta Cryst.* C**48**, 703–706.